INTERNATIONAL JOURNAL OF HYDROGEN ENERGY 39 (2014) 15786–15802

Available online at www.sciencedirect.com

ScienceDirect

journal homepage: www.elsevier.com/locate/he

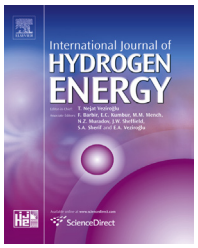

In-cylinder investigations and analysis of a SI gas engine fuelled with H_2 and CO rich syngas fuel: Sensitivity analysis of combustion descriptors for engine diagnostics and control

Anand M. Shivapuji [1], *S. Dasappa* [*]

Center for Sustainable Technologies, Indian Institute of Science, Bangalore 560012, India

ARTICLE INFO

Article history:
Received 11 June 2014
Received in revised form
19 July 2014
Accepted 22 July 2014
Available online 16 August 2014

Keywords:
Syngas
Combustion phasing
Combustion descriptors
Knock detection
Engine diagnostics

ABSTRACT

The sensitivity of combustion phasing and combustion descriptors to ignition timing, load and mixture quality on fuelling a multi-cylinder natural gas engine with bio-derived H_2 and CO rich syngas is addressed. While the descriptors for conventional fuels are well established and are in use for closed loop engine control, presence of H_2 in syngas potentially alters the mixture properties and hence combustion phasing, necessitating the current study. The ability of the descriptors to predict abnormal combustion, hitherto missing in the literature, is also addressed.

Results from experiments using multi-cylinder engines and numerical studies using zero dimensional Wiebe function based simulation models are reported. For syngas with 20% H_2 and CO and 2% CH_4 (producer gas), an ignition retard of 5 ± 1 degrees was required compared to natural gas ignition timing to achieve peak load of 72.8 kWe. It is found that, for syngas, whose flammability limits are 0.42–1.93, the optimal engine operation was at an equivalence ratio of 1.12. The same methodology is extended to a two cylinder engine towards addressing the influence of syngas composition, especially H_2 fraction (varying from 13% to 37%), on the combustion phasing.

The study confirms the utility of pressure trace derived combustion descriptors, except for the pressure trace first derivative, in describing the MBT operating condition of the engine when fuelled with an alternative fuel. Both experiments and analysis suggest most of the combustion descriptors to be independent of the engine load and mixture quality. A near linear relationship with ignition angle is observed. The general trend(s) of the combustion descriptors for syngas fuelled operation are similar to those of conventional fuels; the differences in sensitivity of the descriptors for syngas fuelled engine operation requires re-calibration of control logic for MBT conditions.

* *Corresponding author*. Tel.: +91 9845598203.
E-mail address: dasappa@cgpl.iisc.ernet.in (S. Dasappa).
[1] Tel.: +91 9448775050.

http://dx.doi.org/10.1016/j.ijhydene.2014.07.122

Introduction

Ignition timing is one of the most important control parameters in the operation of a spark ignited (SI) engine. The standard procedure is to set the spark timing to achieve maximum or knock limited brake torque while exercising control over parameters like emissions, etc. The maximum brake torque (MBT) ignition timing is a function of progress of combustion [1] and is influenced by parameters like fuel/mixture thermo-physical property, boost pressure, engine speed and ambient conditions. Perturbations in any of these parameters would require tuning of ignition timing to maintain MBT operation. Historically, tuning of ignition timing has been through lookup table based open loop control systems [2]. These being deterministic at best [3,4], are making way for stochastic closed loop systems that (predominantly) use in-cylinder pressure trace derived information as a control parameter [5,6]. A review of the literature indicates that, under MBT ignition settings, pressure-crank angle profiles and their derivatives (like heat release and mass burn fraction traces) attain inflection characteristics at fixed crank angles and deviation from these angles suggest **OFF MBT** operation. With the chemical to mechanical energy conversion being through the four bar mechanism in internal combustion engines, the crank-connecting rod assembly dictates the position of pressure trace derived parameters. The pressure trace derived inflection parameters are known as combustion descriptors [7] as they quantify phasing of the combustion process in relation to crank angle. Stochastic control systems use the deviations in combustion descriptors from MBT reference values to tune the ignition timing to re-position the engine operation at MBT.

A number of combustion descriptors have been proposed [7]. The position of peak pressure (PoPP) reported by Hubbard et al. [2], is potentially the most widely used descriptor. Hubbard reports that the PoPP is always located around 15° after top dead center (TDC) for MBT operation while Heywood [1] reports 16° after TDC for similar conditions. Cook et al. [8], suggested that the crank angle corresponding to the maximum of the pressure trace first derivative i.e., position of peak pressure rise (PoPPR) is positioned around 3 degrees after TDC for MBT operation. Similarly, it is reported that the position of 50% mass burn fraction (PoMBF50) [9–11] and position of maximum heat release (PoMHR) [7,12], both derived from in-cylinder pressure trace [13,1] are around 9° after TDC for MBT operation. Matekunas [14–16] has introduced a pressure ratio based descriptor, PRM10 (for pressure ratio management at 10° after TDC), and suggested a value of 0.55 for MBT operation. The descriptor PRM10 is significant considering that it is based fundamentally on non intrusive pressure pickup which has significant obvious advantages [17,18]. Literature reported magnitudes of the identified combustion descriptors for MBT ignition setting are consolidated in Table 1. It may be noted that, around 10° after TDC, the piston acceleration picks up and it is in this regime that most of the combustion descriptors are required to be positioned for MBT operation making the kinematic influence explicitly evident.

Table 1 – Comparison of producer gas descriptors at MBT with literature reported values.

	PoPP (degrees)	PoMBF50 (degrees)	PoMHR (degrees)	PRM10
Magnitude	14–16	~9	~9	0.55
Reference	[1,2,5]	[9–11]	[7,12]	[14]

The descriptors and their magnitudes listed in Table 1 quantify the MBT combustion phasing for engine operation with conventional high calorific value fuels like gasoline and natural gas (NG). With increasing use of alternative fuels in internal combustion engines designed for conventional fuels (due to limited availability of dedicated non-fossil fuel engines), evaluation and sensitivity analysis of combustion descriptors becomes critical due to the substantial differences in the thermo-physical properties between conventional and alternative fuels [19]. The differences in thermo-physical properties reflect on the heat release and pressure evolution pattern in the engine cylinder, cumulatively influencing the overall combustion phasing and hence the descriptors. The need for such an analysis becomes critical if the considered alternative fuel contains H_2. Presence of hydrogen in the mixture leads to an increase in the mixture laminar flame speed [20] and enhanced heat loss from the engine due to higher thermal diffusivity [21,22] and smaller flame quenching distance [23]. Hydrogen also influences the turbulent flame structure and propagation speed by inducing flame instability due to preferential diffusion and cellularity [24,25]. The collective influence H_2 on combustion phasing can thus be substantial, requiring detailed investigation.

The present work reports on the systematic study of combustion descriptors for syngas with a composition typical of producer gas (PG), an H_2 and CO dominant bio-derived gaseous alternative fuel. Motivation for the current work arises from the fact that combustion phasing for producer gas differs substantially from that of conventional fuels. The full details describing the difference in heat release pattern between producer gas and conventional fuels is presented by the authors elsewhere [26]. Further, being an in-situ fuel gas generation process, producer gas composition and energy content are susceptible to variations with time, motivating the current study. A review of the literature indicates no discussion dealing with combustion phasing for producer gas fuelled engine operation, further justifying the current intervention.

In the present work, combustion phasing for producer gas fuelled operation is addressed based on experimental investigations and numerical studies. The experimental investigation involved the operation of a six cylinder gas engine with producer gas towards establishing the;

- MBT timing and peak load for naturally aspirated (NA) and turbocharged (TA) operation
- rich, lean and optimal mixture quality
- operating regime for NA and TA mode and
- knock regimes

Numerical analysis involved the development and use of a first law based zero dimensional (0D) model [26] for parametric sensitivity analysis on;

- ignition timing
- load variations and
- mixture quality

Having addressed producer gas fuelled operation in detail, the analysis is extended to a address the influence of hydrogen fraction in syngas on the combustion phasing, especially in terms of the sensitivity of the descriptors to ignition angle. Four different syngas compositions have been considered for addressing the influence of H_2 fraction on combustion phasing.

Sensitivity analysis

The robustness of a control system is fundamentally a strong function of the stability and sensitivity of the underlying control logic. While the control systems are designed to accommodate perturbations in input parameters, a behavioural shift in the system response calls for re-calibration of the governing logic to accommodate phase and response alterations. This requires a detailed sensitivity analysis involving the assessment of system response to variations in the control input parameters. For the current work, with an aim of extending the philosophy of combustion descriptor based engine control established for conventional high calorific fuels to syngas operation, a detailed sensitivity analysis addressing the influence of specific operational parameters on the in-cylinder combustion phasing becomes critical. The sensitivity analysis seeks to quantify the variations in combustion descriptors with parametric perturbations on fuelling with syngas to access the need for control logic re-calibration.

With the variations in thermo-physical properties of the fuel on fuelling the engine with syngas, the heat release and in-cylinder pressure trace are expected to be phased differently as compared to conventional fuels and the phasing/profile alteration with parametric perturbations is expected to differ significantly. Accordingly, a significant change in the descriptors sensitivity is expected. In light of the above, the sensitivity of combustion descriptors to mixture quality, load, and ignition timing is addressed both numerically and through experimental investigations.

Combustion phasing sensitivity analysis : simulation studies

Numerical sensitivity analysis is carried out using a first law based zero-dimensional model where the heat addition is by a cumulative distribution Wiebe function [27] described in equation (1). Detailed description of the Wiebe function

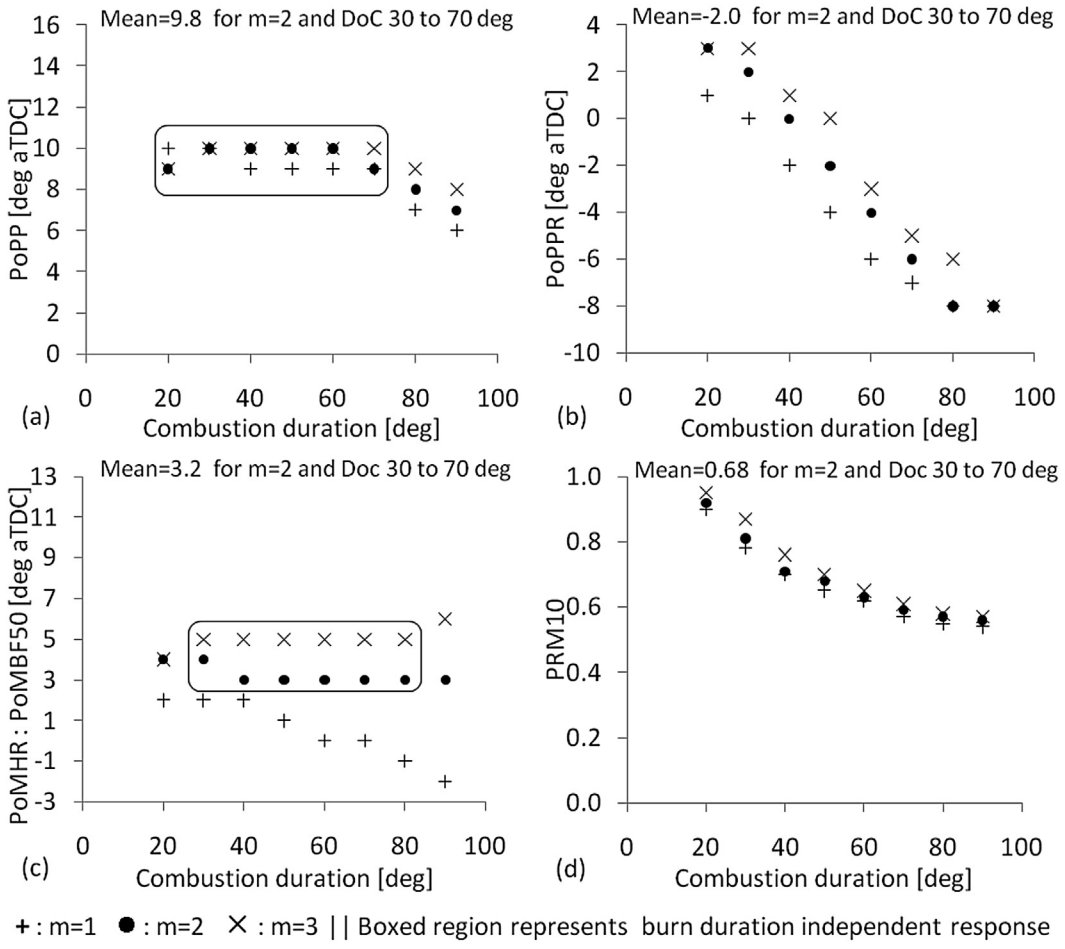

Fig. 1 – Sensitivity of combustion descriptors to heat release pattern and duration.

based 0D model has been reported by the authors elsewhere [26].

$$\frac{Q_{chem}(\theta)}{Q_{chem-total}} = 1 - exp\left[-a\left(\frac{\theta-\theta_{soc}}{\Delta\theta}\right)^{m+1}\right] \quad (1)$$

In the Wiebe function, the combustion duration ($\Delta\theta$), the shape factor (m), start of combustion angle (θ_{soc}) and the cycle heat input ($Q_{chem-total}$) are tuned to represent the variation in ignition angle, load and mixture quality. The parameters range covering different scenarios for a variety of fuels (fossil and non-fossil) [28,23,29,30] are as below;

- Cycle energy input variation between **500 and 1500 J/cycle**. The cycle energy input variation represents the engine operation between part load and full load conditions.
- Ignition angle variation between **−60 degrees and 0 degrees before TDC.** The ignition angle is tuned depending on the in-cylinder flame propagation rate which depends on the laminar flame speed (representative of fuel thermo-physical property) and the in-cylinder turbulence (representative of in-cylinder fluid motion). The indicated range thus simultaneously accounts for the variation of laminar flame speed and in-cylinder turbulence.
- Shape factor variation between **1 and 3**. The shape factor is a representative of the cumulative heat release pattern in the engine and accommodates the heat released due to combustion of the mixture (representative of in-cylinder mixture energy density) and the heat lost to the engine walls (representative of in-cylinder temperature and convective heat transfer coefficient).

Sensitivity to mixture quality

The quality of the mixture in the engine cylinder, quantified in terms of operating equivalence ratio, has a significant impact on the in-cylinder heat release and pressure profile. The variation of the position of peak pressure, position of peak pressure rise, position of maximum heat release, position of 50% mass burn fraction and pressure ratio management at 10° after TDC for MBT ignition (identifying by comparing $W_{indicated} = \int PdV$ at different ignition angles) for three different shape factors of 1,2 and 3, representing mixture quality variations, are plotted as a function of combustion duration in Fig. 1(a)–(d) respectively. Effectively, each figure while explicitly describing the variation of individual descriptor with combustion duration, also describes the influence of the shape factor. The PoMHR and PoMBF50 are clubbed together since the trend/response was almost overlapping. The average value of the descriptors for the combustion duration ranging from 30 to 70 degrees crank angle for $m = 2$, representing the range for operation with conventional fuels [1] is included as inset data.

Some of the key observations from Fig. 1 are consolidated as below;

- PoPP and PoMHR/PoMBF50 are broadly independent of the combustion duration. The average values are around 9° and 4° after TDC respectively, about 5° advanced as compared to respective literature reported MBT values.
- PoPPR indicates near linear dependence to combustion duration with very high sensitivity.
- PRM10 is mostly independent of the shape factor with a non-linear sensitivity to combustion duration. The average value is higher by over 20% as compared to around 0.55 reported in the literature.

It is interesting to note that, while PoMHR and PoMBF50 indicate sensitivity to the shape factor, PoPP and PRM10 are almost completely independent.

Sensitivity to load

An engine can operate at full or part load depending on the prevailing demand. Load dependence of in-cylinder heat release and pressure profile is through the variation (increase) in the turbulence and temperature, especially of the unburned mixture. Sensitivity of the descriptors to load, presented in Fig. 2(a), is addressed by varying the cycle energy input. For brevity, the results are restricted to shape factor of 2 and combustion duration of 50°.

Some of the key observations from Fig. 2(a) are consolidated as below;

- PoMHR/PoMB50 and PRM10 remain independent of load over the entire range
- For input greater than 1000 J/cycle (typical power generation cycles), PoPP is independent of load
- PoPPR indicates near linear load dependence.

The indicated results hold for all the shape and efficiency factors within ±0.5° for angle based descriptors and ±0.025 for PRM10. It may be noted that while Wiebe based model is inherently not capable of handling variations in turbulence (hence zero dimensional) and also temperature, the same gets

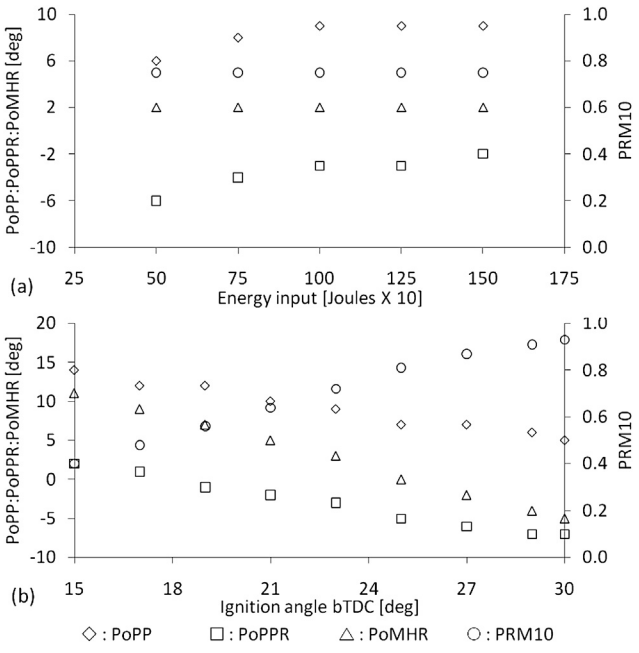

Fig. 2 – Sensitivity of combustion descriptors to (a) load and (b) ignition angle.

Table 2 – Comparison of thermophysical properties of producer gas with convention fuels.

	Gasoline	H_2	CH_4	PG[a]
Air-Fuel ratio (kg/kg) at $\phi = 1$	14.7	34.3	17.0	1.30
Fuel lower calorific value (MJ/kg)	44.4	121	50.2	5.00
Mixture calorific value (MJ/kg) at $\phi = 1$	2.82	3.42	2.78	2.17
Product to reactant mole ratio at $\phi = 1$	1.05	0.85	1.00	0.90
Flame speed (m/s) at $\phi = 1$	0.41	2.37	0.42	0.50
Adiabatic flame temperature (K) at $\phi = 1$	2580	2480	2214	1873

[a] Composition – CO and H_2 19%, CH_4 1.8%, CO_2 9.0%, balance N_2.

0 accounted when the shape factor and combustion duration are altered. Thus, the above results unequivocally establish the load independence of the combustion descriptors.

Sensitivity to ignition timing

Sensitivity of the descriptors to ignition timing is addressed by varying the ignition timing 10° (in steps of 1°) on either side of MBT ignition angle for typical liquid fuels. The considered ignition angle range is primarily indicative of the mixture laminar flame speed. It is important to note that, the variation in ignition angle is for a given shape factor and combustion duration since the idea is to address the influence of ignition angle on the descriptors.

It is evident from Fig. 2(b) that the descriptors are linearly dependent on the ignition angle. The pressure trace derived descriptors shift towards the TDC on advancing the ignition while the magnitude of PRM10 increases and vice versa. With ignition advance, the pressure profile and hence the angle based descriptors are positioned closer to the TDC. Correspondingly, with an increase in the firing pressure at 10° after TDC, the magnitude of PRM10 increases.

Combustion phasing sensitivity analysis: experimental investigations

The fuel: syngas

Bio derived syngas is generated from thermo-chemical conversion of biomass in a gasifier [31]. Air gasification is used to generate syngas of a particular composition, known as producer gas with composition (dry) of 19 ± 1% H_2, 19 ± 1% CO, 1.8 ± 0.4% CH_4, 9.0 ± 1% CO_2 and balance N_2 and has a lower calorific value (LCV) of 4.9 ± 0.2 MJ/kg. For generating syngas of varying H_2 fraction, an oxy-steam gasifier is used where air as the gasifying media is replaced by oxygen and steam and the steam to biomass ratio is adjusted to obtain the desired H_2 fraction [32].

The thermo-physical properties of producer gas [33,34] are compared with those of conventional fuels in Table 2.

Table 3 – Syngas compositions (varying H_2 fraction) adopted in the current work.

	C1	C2	C3	C4
Composition				
Carbon monoxide (%)	11.5	18.0	14.4	16.4
Hydrogen (%)	12.8	18.0	25.9	37.2
Methane (%)	2.3	1.2	2.9	3.6
Carbon dioxide (%)	10.8	11.3	19.0	24.7
Nitrogen (%)	62.6	51.5	37.8	18.1
Thermo-physical properties				
Fuel LCV (MJ/kg)	3.14	4.17	5.28	7.55
Stoichiometric A/F (kg/kg)	0.88	1.12	1.49	2.14
Mixture LCV (MJ/kg)	1.67	1.97	2.12	2.41
Thermal diffusivity (cm^2/s)	0.302	0.339	0.383	0.455

Differences in thermo-physical properties, with potential to influence the combustion phasing are explicitly evident.

The four syngas compositions used in the current study towards addressing the influence of H_2 fraction on combustion phasing are consolidated along with some basic thermo-physical properties in Table 3 below.

Engine and instrumentation

Two multi-cylinder engines (two and six cylinders), both of Cummins India Limited make, are used in the current analysis. The two cylinder engine is available as a commercial naturally aspirated diesel engine while the six cylinder engine is available as a commercial naturally aspirated/turbocharged NG engine derived from diesel frame. The engine specifications are listed in Table 4. The in-cylinder pressure is measured using an AVL make spark plug adapted un-cooled, piezo-electric, differential pressure sensor (GH13Z) at an acquisition frequency of 90 kHz. Differential to absolute conversion is by using a manifold pressure sensor with a reference pressure supplement.

Uncertainty analysis

Uncertainties are inherent in any experimental measurement and when such measured values are combined in some mathematical function towards the estimation of a desired

Table 4 – Specifications of the engine.

Six cylinder engine	
Engine make and model	Cummins India Limited – 6B5.9
Rated output (Turbocharged)	90 kWe on diesel and 76 kWe on NG
Displacement	5.9 L
Engine speed	1500 rpm
Compression ratio	16.5 in CI mode and 10.5 in SI mode
Two cylinder engine	
Engine make and model	Cummins India Limited – X 1.7 G1
Rated output (Naturally aspirated)	15 kWe on diesel
Displacement	2.3 L
Engine speed	1500 rpm
Compression ratio	18.5 in CI mode and 11.0 in SI mode

parameter, the calculated parameter itself also will have some uncertainty. As such uncertainty analysis becomes essential to quantify the degree of confidence associated with calculated results. In the current analysis, the uncertainty is communicated with respect to the systematic errors and towards the same, the range and accuracy of the instruments used in the current analysis are listed in Table 5 below.

The uncertainty analysis is based on the methodology developed by Kline and McClintock [35,36] wherein the information about uncertainties in individual measurements is used to estimate the uncertainty associated with the calculated parameter. If **C** is a parameter that is calculated using experimentally measured values $E_1,E_2,\ldots E_n$ and $e_1,e_2,\ldots e_n$ are the corresponding uncertainties associated with each of the measurements, then the uncertainty (c_u) associated with the calculated value C for the function of the type.

$$C = C(E_1, E_2, \ldots.) \tag{2}$$

is estimated using the following expression;

$$c_u = \sqrt{\left(\frac{\delta C}{\delta E_1} * e_1\right)^2 + \left(\frac{\delta C}{\delta E_2} * e_2\right)^2 + \ldots + \left(\frac{\delta C}{\delta E_n} * e_n\right)^2} \tag{3}$$

Care must be exercised in the use of equation (3) in that the individual measurement uncertainties (e_i) are the absolute values and not the percent uncertainty generally reported. The uncertainty (in absolute numbers) corresponding to peak value for the parameters relevant for the current investigation are tabulated in Table 6 as below;

The uncertainties associated with the parameters indicated in Table 6 are well within the values reported in literature [37–39].

Methodology

Experimental investigations involved operating the engine under naturally aspirated (NA) and turbocharger after-cooled (TA) mode. Spark sweep test establishes the MBT spark timing. At MBT ignition, the engine was operated from zero to full supported load in steps. At each load, the mixture quality was varied (overriding carburettor settings for stoichiometric operation) to identify the rich and lean limit. Abnormal combustion in the engine was initiated by increasing the mixture temperature in the inlet manifold by controlling water flow rate through the after-cooler. At each of the operating conditions discussed above, in-cylinder pressure traces of 750 consecutive cycles were acquired in three batches.

In the current analysis sensitivity of the descriptors to load, ignition angle and mixture quality has been addressed considering that, for a typical power generation system, these are the influencing parameters. Being a production engine connected to an alternative current generator, no provision for changing the CR and the engine speed was available. Hence sensitivity to CR and speed has not been addressed.

Table 5 – Range and accuracy of the instruments used.

Instrument	Range	Accuracy
Fuel gas analyser		
CO	0–100%	±0.05%
H_2	0–100%	±0.05%
CH_4	0–100%	±0.05%
CO_2	0–100%	±0.05%
O_2	0–025%	±0.005%
Cylinder pressure	0–150 bar	±0.5 bar
Angle encoder		±0.25 deg
Venturi (C_d)		±1.0% (full scale)
Manometer		±1.00 mm
Engine speed	0–20,000 rpm	±10 rpm
Temperature	−200 to 1250 °C	greater of 2.2 °C/0.75%
Watt-meter	0–100 kW	±1.0%

Table 6 – Calculated value uncertainty.

Parameter	Peak value	Uncertainty
Power (kW)	75.0	±1.00
Gas LCV (MJ/kg)	04.9	±0.25
Gas flow (kg/h)	197.0	±1.55
Air flow (kg/h)	216.0	±1.65

Experimental results

Spark sweep test

Spark sweep test using syngas indicated the MBT ignition timing at 24 and 22° before TDC for NA and TA mode respectively; retarded by 4 and 6° with respect to corresponding NG MBT settings. The ignition retard is attributed to higher flame speed for producer gas as compared to NG (refer Table 2) and flame cellularity introduced by H_2 [40,41]. The additional 2° retard for TA mode is attributed to higher turbulence in TA mode [42,43].

Peak supported load

The peak supported load on the engine is at 27.3 kWe for NA mode and 72.8 kWe at compressor pressure ratio of 2.2 under TA mode of operation. The NA mode peak load is limited by cyclic variations and engine de-speeding while the TA mode peak load is knock limited. Engine knock beyond 72.8 kWe is evident from the heat release and pressure crank angle traces in Fig. 3.

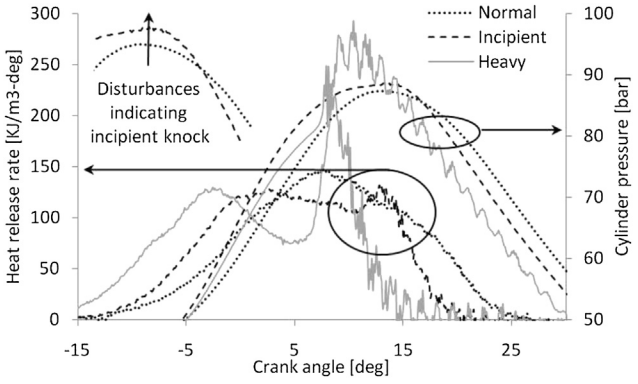

Fig. 3 – Pressure crank angle and heat release traces at peak load and beyond.

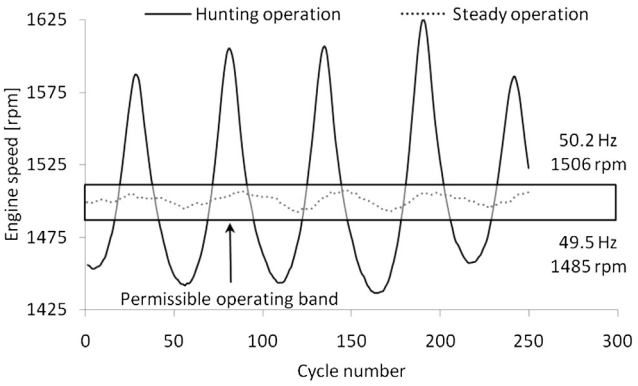

Fig. 4 – Engine response to lean mixture operation.

Power de-rating to the tune of 17 kWe under TA mode is not unexpected. Dasappa [44], in the work on estimation of power from diesel engines converted for gas operation, has established that, for every unit reduction in CR, the peak load drops between 1% and 3% of the original rating. With a drop in CR by 6 units (from 16.5 to 10.5) and considering a power loss factor of 3%, the expected de-rating is 18 kWe. Complete details regarding the energy balance and de-rating of the engine used in the current analysis have been discussed by the authors elsewhere [45].

Operating mixture quality limit

In order to address the effect of mixture quality on the engine performance, the rich and lean limit mixture quality supported by the engine at different loads and fixed MBT ignition timing are established.

Lean operating limit

On approaching the lean limit, an overall increase in the combustion duration and cyclic dispersion in heat release [46] is observed due to higher flame kernel formation and turbulent flame propagation time scales. These factors collectively lead to combustion instabilities [47] manifesting as fluctuations in torque and increased emissions. Many different approaches, primarily based on in-cylinder analysis like first engine misfire [48], the total number of misfires [49], variations in the IMEP [1,50] etc., and exhaust analysis for certain specie threshold concentration have been suggested for identifying the lean operational limit.

In the current analysis, for power generation applications, fluctuations in engine speed (and hence alternator frequency) has been considered as the limiting condition for lean operation. Engine speed fluctuation as a parameter to indicate the lean limit is chosen since speed can be monitored without in-cylinder instrumentation. The permissible engine speed (alternator frequency) fluctuation band of 1485 rpm (49.5 Hz) and 1506 rpm (50.2) Hz (Indian standards) as specified in the Indian Electricity Grid Code [51] has been considered for establishing the lean limit. Fig. 4 presents the variation of the engine speed for 250 consecutive cycles when the engine is operated with a lean mixture. It is observed that, up to a threshold (lean) limit, fluctuations are well within the specified band and when mixture becomes leaner than the threshold, fluctuations become extremely large.

Rich operating limit

As the mixture is made fuel rich, beyond the threshold limit, minor intermittent discrepancies on pressure profiles begin to appear. With further increase in the fuel-air ratio, the discrepancies become more prominent and occur with increasing frequency tending towards well established

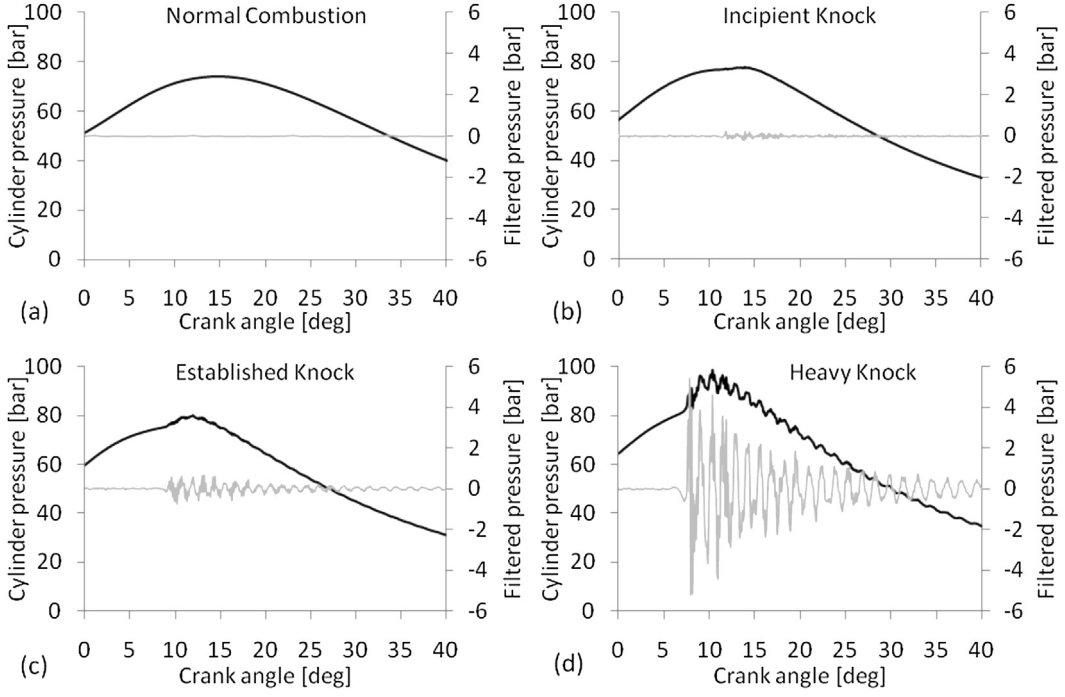

Fig. 5 – Normal to knocking combustion transition.

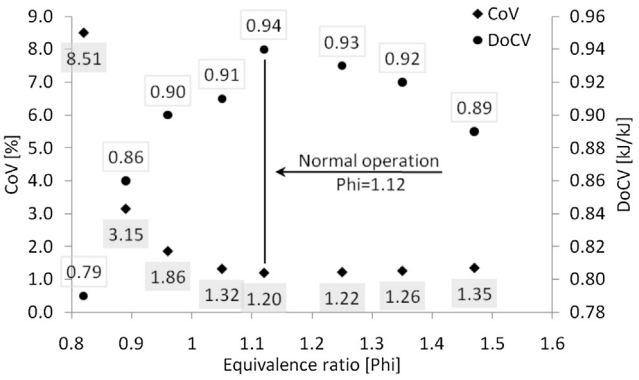

Fig. 6 – Variation of IMEP and DoCV combustion with mixture quality at 40 kWe load.

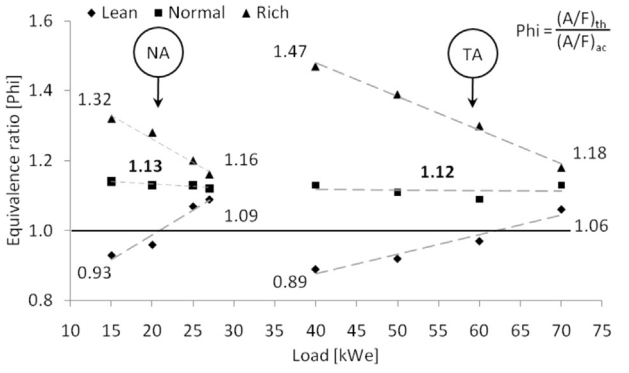

Fig. 7 – Operating regime for NA and TA mode of operation.

knocking operation. Fig. 5 presents the transition of engine operation from normal to a heavy knock as recorded in the current investigation.

In the current analysis, the first appearance of minor discrepancies in 250 consecutive cycles is considered as the limiting condition within which engine operation is considered to be knock free. Detection of incipient knock from visual observation of pressure traces is difficult (being qualitative) especially while monitoring consecutive cycles. Towards this end, each pressure trace is subjected to online low pass filtration (4 kHz) to remove the base curve and retain only the high frequency component. The high frequency component is further subjected to spectral analysis. The shock wave generated from end gas auto-ignition is known to excite characteristic frequencies in the range of 5 kHz–7 kHz that represents the natural vibration of the first order transverse mode of the gas. Presence of frequency in this band is a well established method of identifying knock [1,52,53].

Optimal operating mixture quality

While the rich and lean limits represent permissible extremities, the engine has to be operated at an optimal mixture quality at which the overall engine response is at its best. Towards identifying the optimal operating condition, coefficient of variation (CoV) of IMEP at various equivalence ratios was evaluated. The CoV of IMEP is an important indicator of combustion stability in an engine [1,54] and is frequently used as a parameter to quantify stable engine operation with minimum fuel consumption [21,47,55].

Fig. 6 presents the CoV of IMEP (shaded data labels) as a function of mixture quality at 40 kWe load under TA mode of operation. It is observed that, at extreme lean mixture quality, the CoV in IMEP is as high as 8.51 and reduces as the mixture gets fuel rich. The CoV of IMEP attains a minimum at $\phi = 1.12$. As the mixture is made rich beyond $\phi = 1.12$, the CoV of IMEP tends to increase, albeit marginally, making it difficult to fix $\phi = 1.12$ as the optimal operating mixture quality. Towards resolving this issue, another important pressure trace based parameter, the degreesree of constant volume (DoCV) [56] is evaluated. The DoCV is a relative measure of the extent of deviation from a typical constant volume cycle. Higher the DoCV better is the cycle in terms of efficiency of energy conversion. The DoCV is mathematically expressed as;

$$\xi = \frac{1}{\eta_{otto} Q_{cum}} \int \left[1 - \left(\frac{V_s + V_c}{V(\theta)}\right)^{1-\gamma}\right] \frac{dQ}{d\theta} d\theta \quad (4)$$

Variation of DoCV with ϕ is indicated in Fig. 6 (bordered data labels). It can be observed that DoCV increases on moving away from the limiting mixture quality and reaches a maximum at $\phi = 1.12$. Simultaneous comparison of IMEP and DoCV variation with equivalence ratio indicates ϕ of 1.12 as the optimal mixture quality at 40 kWe under TA mode of operation. Similar exercise is carried out at the other loads for both NA and TA operation and the corresponding optimal mixture quality is identified.

Operating regime for NA and TA mode of operation

Having identified the criterion for establishing the lean, rich and optimal operation equivalence ratio, the mixture quality operating regime of the engine for producer gas fuelled operation is presented in Fig. 7 for both NA and TA mode of operation.

One of the key features of the mixture quality operating regime is that the optimal operating ϕ over the entire load range and the whole regime (rich to lean) at higher loads (>70%) is positioned with ϕ greater than unity. The optimal operation mixture quality is of significant interest considering that, for the greater part of its operational life, the engine will be fuelled with mixture corresponding to $\phi = 1.12$. The rich mixture quality for optimal operation can be addressed by

Table 7 – Peak laminar flame speed and corresponding equivalence ratio for different CO–H_2 mixtures.

	Carbon monoxide - hydrogen ratio in the fuel						
Composition	20–80	30–70	40–60	50–50	60–40	70–30	80–20
Flame speed (cm/s)	313.7	290.7	263.5	233.2	199.3	169.4	136.3
Equivalence ratio	1.9	2.0	2.1	2.3	2.5	2.7	3.0

Table 8 – Variation in descriptor for set power loss band.

% Drop	PoPP (degrees)	PRM-10
±2.5	±0.2	±0.01
±5.0	±0.5	±0.04

analysing the influence of relevant thermo-physical properties on the CoV of IMEP and DoCV. It is well established that shorter combustion duration leads to reduced cyclic variations [21,57] while equation (4) indicates that shorter combustion duration leads to higher DoCV. Accordingly, the parameter that influences the combustion duration i.e., the laminar flame speed is analysed by identifying the laminar flame speed of producer gas-air mixture as a function of ϕ. The PREMIX module of CHEMKIN [58] is used for the estimation of laminar flame speed as a function of ϕ for atmospheric conditions (1 bar, 300 K) and engine like conditions (25.4 bar, 716 K). Assessment of the data indicates that for producer gas (20% CO and H_2, 2% CH_4, 12% CO_2 and balance N_2) the laminar flame speed peaks on the rich side of stoichiometry at ϕ of 1.3 (atmospheric) and 1.2 (engine) for the tested conditions, justifying the need for a rich mixture quality for optimal engine operation.

The laminar flame speed attaining a peak value towards the fuel rich condition is attributed to the presence of CO and H_2; both of which have peak laminar flame speeds for fuel rich mixtures [59–62]. Table 7 consolidates the equivalence ratio corresponding to the peak un-stretched planar laminar flame speed for various CO–H_2 mixtures for atmospheric conditions. Literature reports that, for fuels containing H_2, rich fuel-air mixtures are highly reactive due to chemical autocatalysis resulting in the regeneration of the reactive H species [63,64]. Hence, the peak flame speeds are observed for richer than stoichiometric mixtures.

Analysis and discussions

This section presents a detailed analysis of the combustion descriptors response to perturbations in the three operating conditions of load, mixture quality and ignition angle for producer gas fuelled operation. The analysis addresses parametric dependencies and the corresponding sensitivities which also serve to validate the finding of numerical analysis. The study also quantifies the differences in the descriptors response when the engine is fuelled with producer gas and fossilized fuels. Response of the descriptors to abnormal combustion is also addressed.

Effect of cycle to cycle variations on combustion descriptors

Typically, an engine experiences cycle to cycle variations, affecting combustion phasing [1,65,66] even when all operating parameters are held constant. Corrective action to the ignition timing using a closed loop control system cannot be based on individual cycle descriptor(s) as it may jeopardize the stability of the control system due to random and oscillatory nature of the input signal. Further, one odd outlier from a slow cycle can trigger the control system to dangerously over advance the ignition timing leading to end gas auto-ignition [1,67].

Recognizing the difficulty associated with the use of individual cycle descriptors for ignition control, two statistical averaging techniques are adopted to generate descriptors representing set of operating condition. In one approach, descriptors are derived from the ensemble average pressure trace while, in the other, descriptors are identified for consecutive cycles and are subsequently averaged. The criterion for determining the number of cycles to be considered for averaging is based on the permissible drop in the peak power (corresponding to MBT ignition) when the average descriptor will be within a band.

A review of the peak supported load against ignition angle in a spark sweep test suggests that for NA and TA mode operation, the maximum loss in power per degree offset in ignition is at about 2.5 kWe or 9% of peak power and 3.2 kWe or 5% of peak power respectively. The deviation from the mean (MBT ignition timing, normal operation ϕ) of PoPP and PRM-10 for ±2.5% and ±5.0% of peak power loss are listed in Table 8 below. The choice of PoPP and PRM-10 is based on the consideration that PoPP is independent of the absolute pressure correction while PRM-10 is dependent on the absolute values. This accounts for absolute pressure correction as a factor. The case of lean operating limit is described because the cyclic variations in combustion phasing are highest for the lean limit (as discussed earlier) and accordingly the number of cycles required for averaging would increase.

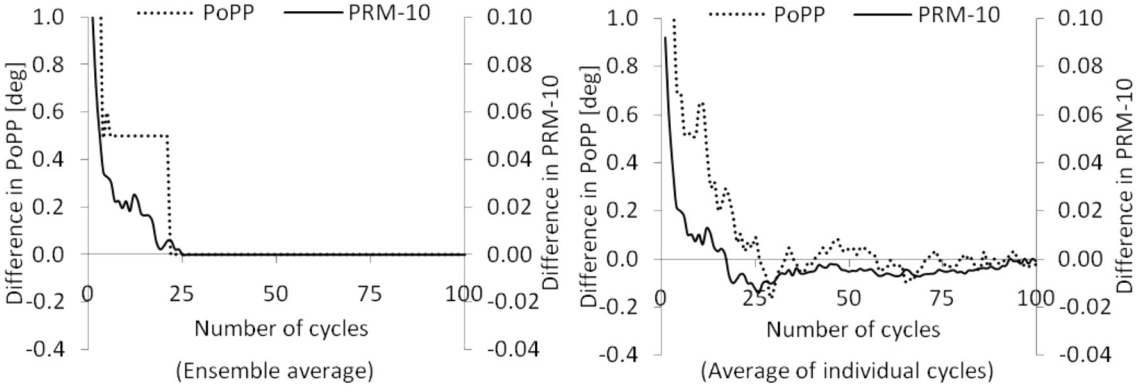

Fig. 8 – Variation of descriptors with number of cycles for averaging.

Table 9 – Skewness in PoPP under NA and TA mode of operation.

Cyl-6	Cyl-5	Cyl-4	Cyl-3	Cyl-2	Cyl-1
Naturally aspirated – 25 kWe					
0.042	−0.194	0.045	−0.007	−0.227	0.021
Turbocharged aftercooled – 70 kWe					
0.023	−0.116	0.025	−0.008	−0.138	0.018

The deviation from 1000 cycles mean for PoPP and PRM-10 as a function of the number of cycles considered is shown in Fig. 8. Analysis of the data as presented in the figure suggests that stability is achieved well within 25 cycles for both ensemble and individual cycle average. In comparing the two methods, it is important to note that, as the permissible band broadens (i.e., allowable power drop is increased) the individual cycle average is superior to the ensemble average. However if the permissible drop from the peak is very narrow like 0.5% then stabilization based on individual cycle averaging requires 93 cycles, significantly large as compared to 25 cycles for ensemble averaging.

While ensemble average based approach caters to a wide spectrum of ignition control and is a logical choice, monitoring individual cycles as required for descriptors averaging, has a distinct added advantage. Outliers, which generally indicate combustion abnormality like misfire or auto ignition can be immediately recognized and corrective action initiated. As an example, in the event of misfire, the PoPP would shift to the TDC while PRM-10 would theoretically be zero. Similarly, in the event of engine knock, the PoPP would be substantially different and PRM-10 abnormally high. Considering that both the methods have certain advantages and limitations, the choice of any one of them becomes case specific. In the current work ensemble average method involving the average of 50 consecutive cycles is adopted.

Assessment of combustion phasing bias in multi-cylinder operation

Factors like variations in quantity and quality of the mixture entering the cylinders, exhaust gas recirculation and possible differences in the cylinder(s) cooling [1] introduce cylinder to cylinder variations in a typical multi-cylinder engine. In adopting a control system based on pressure trace from a single cylinder of a multi-cylinder engine, an assessment of bias in engine cylinders, if any, needs to be addressed. This assumes significance considering that pressure-crank angle trace for any control application would be recorded from only one of the cylinders while any corrective action would affect all the cylinders. In the event of significant bias being observed from cylinder to cylinder, choice of cylinder for data acquisition becomes critical.

Statistical analysis of the PoPP in terms of skewness (representing the extent of displacement of the probability distribution from the mean) for 250 cycles of each of the six cylinders under wide open throttle for NA and TA mode of operation is presented in Table 9. The numbers indicate the physical position of the cylinders in plan view. The firing order for the six cylinders is 1-5-3-6-2-4.

It can be observed that skewness in all the cylinders is significantly low, indicating the absence of any particular bias. In the six cylinders, cylinder 2 and 4 indicate slightly higher skewness. In the TA mode of operation skewness is significantly lower than NA mode operation. Based on this analysis, it can be concluded that the descriptors are independent of the cylinder from which the data is acquired.

Sensitivity of descriptors to load

Sensitivity analysis of descriptors to load becomes critical considering that, with increasing load, the severity of thermo and fluid dynamic conditions inside the engine cylinder increase, influencing the turbulent flame speed and combustion phasing. Fig. 9 presents the variation of combustion descriptors with load under MBT ignition settings. The variations have been quantified by CoV of the descriptors indicated alongside the respective legends.

It is evident from Fig. 9 that, beyond 20 kWe (25% of the peak load), variations in the combustion descriptors except for the PoPPR, are rather minimal (CoV within 4 ± 3%) and reflects as a near linear trend. A linear least square curve for the variation of the descriptors with load is consolidated in Table 10 where the sensitivity, intercept and range of validity for each of the descriptors is indicated along with the range extreme descriptor value obtained from the curve fit equation. As is evident, the sensitivity of all the descriptors to load is nearly negligible, especially so for the position of maximum heat release which remains virtually independent of the load. This response is consistent with the literature reported behaviour for conventional fuels [7]. For PoPPR, the CoV is close to 40% with no particular trend, rendering it is unsuitable as a descriptor. The above analysis establishes the load independence of combustion descriptors for load above 25%. The observations are also consistent with the outcome of load sensitivity analysis using the zero-dimensional model.

Sensitivity of descriptors to ignition timing

Fig. 10 highlights the sensitivity of descriptors to ignition timing at a fixed speed of 1500 rpm and mixture quality corresponding to normal engine operation. Null hypothesis based goodness of fit (R^2) [68] for the linear correlation is presented

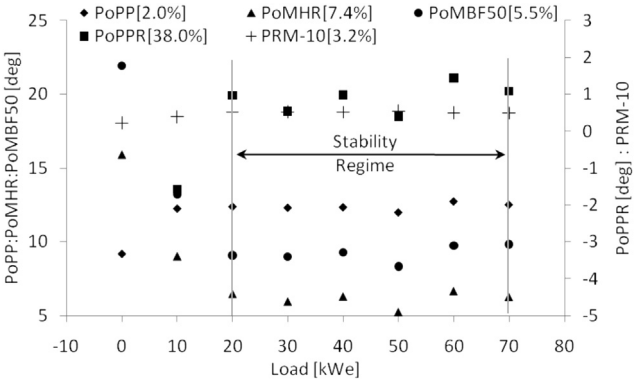

Fig. 9 – Sensitivity of the descriptors to load for TA operation.

Table 10 – Quantification of descriptor sensitivity to load.

Descriptor = [Sensitivity]*Load + Intercept

Descriptor	Sensitivity	Intercept	Range (kWe)		Range magnitude (kWe)	
			Low	High	Low	High
PoPP	+0.00450	12.16	20	75	12.25	12.50
PoMHR	+0.00008	06.16	20	75	06.06	06.17
PoMBF50	+0.01427	08.16	20	75	08.45	09.23
PRM10	−0.00052	00.54	20	75	00.53	00.50

as inset data. Legends around the data points correspond to MBT ignition timing descriptor magnitude for respective fuel/mode of operation.

The descriptors for producer gas fuelled operation under NA and TA mode of operation are compared with descriptors for NA mode gasoline operation. An important feature is that the magnitude of the angle based combustion descriptors under producer gas fuelled TA mode MBT operation remains consistently lower than corresponding gasoline mode values while PRM10 remains higher than gasoline fuelled values over the complete crank angle sweep. This is also evident from the particular values of descriptors at MBT ignition timings as consolidated in Table 11. Current observation of closer to TDC positioning of descriptors at MBT is in-line with the zero-dimensional model results though the magnitudes are slightly different. The difference in the magnitudes can be attributed to the simplicity of the considered model.

Values of descriptors closer to TDC for producer gas operation in comparison with literature reported values for gasoline indicates an altered and advanced phasing of combustion. Difference in position of descriptors is attributed to the presence of H_2 in producer gas-air mixture which enhances the turbulent flame propagation as described in Section The fuel: syngas. Considering PRM10, it can be observed that while the value remains higher than gasoline operation, MBT specific value is lower by about 10% compared to the reported value in literature. PRM10 is a strong function of the pressure at 10° aTDC and any reduction in peak pressure leads to lowering of PRM10. In a work quantifying engine de-rating with producer gas fuelled operation, Dasappa [44] clearly mentions that the peak in-cylinder pressure in the engine will be lower with producer gas fuelled operation even at similar SEC. This is attributed to the lower AFT and lower than unity product to reactant mole ratio and as such the PRM10 is lower.

When considering NA mode operation, the values of PoPP and PRM10 remains lower than gasoline fuelled operation. For PoMHR and PoMBF50 the NA and gasoline dataset cross each other on the advanced side of sparking. Such behaviour is explained comparing the rated output of the engine in NG operation with that of producer gas operation where the peak delivered load in producer gas is about 37.5% of that of NG mode. This reinforces the observation made in the previous section regarding load dependence of descriptors at low loads.

It is evident from Fig. 10 that all descriptors vary linearly with respect to ignition angle. Further, least square curve fit

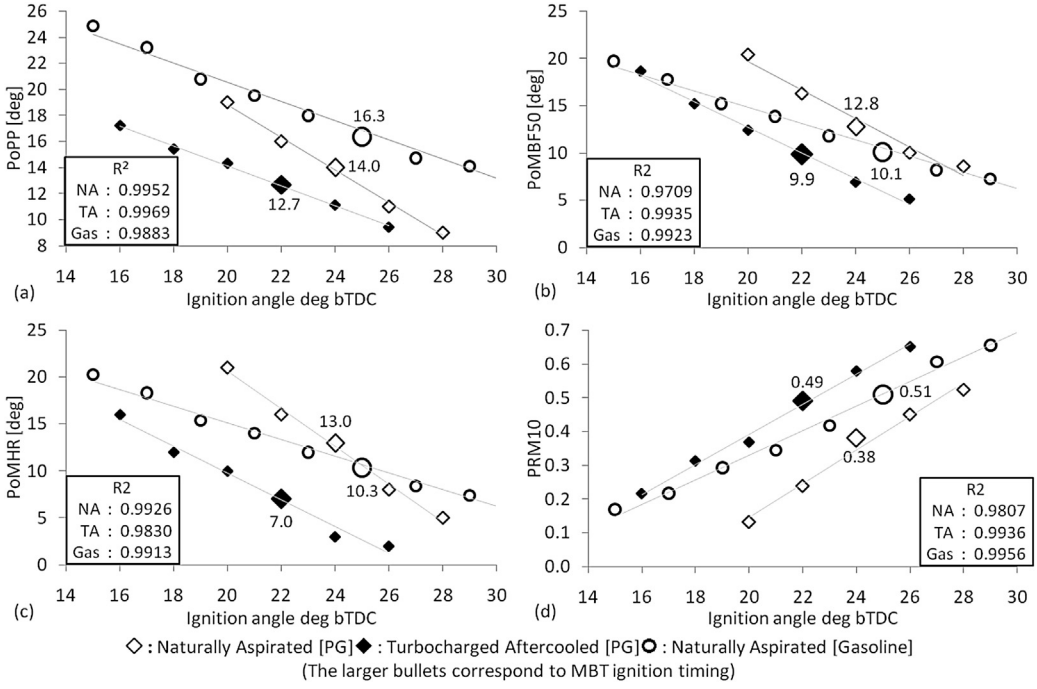

Fig. 10 – Sensitivity of descriptors to ignition angle.

Table 11 – Comparison of producer gas descriptors at MBT with literature reported values.

	PoPP (degrees)	PoMBF50 (degrees)	PoMHR (degrees)	PRM10
PG-NA	14.0	12.8	13.0	0.38
PG-TA	12.7	9.90	7.00	0.49
Gasoline	16.3	10.1	10.3	0.51
Standard	14–16	~9	~9	0.55

indicates a goodness of fit greater than 0.97, consistent with gasoline operation [7]. Slopes (sensitivity coefficient) of linear least square curve fit for producer gas fuelled NA and TA mode of operation along with gasoline operation are consolidated in Table 12. A comparison of the sensitivity is also presented.

It is evident from the tabulated data that, sensitivity to ignition timing is highest for producer gas fuelled NA mode followed by TA mode. Gasoline operation indicates least sensitivity. Further, producer gas fuelled TA mode sensitivity is closer to gasoline operation as compared to NA mode operation. The closeness of TA mode operation to gasoline fuelled operation can be attributed to the fact that, for TA mode, the specific energy consumption (SEC) approaches that of gasoline fuelled operation. Typical measurements indicate that the SEC for gasoline fuelled operation is around 13.5 MJ/kWh while it is 19.5 MJ/kWh and 16.5 MJ/kWh for producer gas fuelled NA and TA mode of operation respectively. An interesting inference that could be drawn is that the engine response in terms of combustion descriptors for alternative fuels approaches fossil fuel operating conditions when the total energy input approaches that of fossil fuels.

Sensitivity of descriptors to mixture quality

Having established the response of the descriptor to load and ignition timing, sensitivity to mixture quality is addressed at two loads of 30 and 50 kWe under turbocharged mode of operation. Response of the four descriptors to mixture quality at the two loads is indicated in Fig. 11.

Fig. 11 suggests that, at higher loads, scatter for angle based descriptors is less than 0.5°. At low loads, a linear trend with close to zero slope (except for PoMBF50) indicates near independence of the descriptors to mixture quality. Further, long duration measurements on the gasification system have indicated the variation in the equivalence ratio due to changes to the gas composition to be within ±0.1. In the ±0.1 range about the normal operation mixture quality (Section Optimal operating mixture quality), it can be observed that, in absolute terms, the deviation in the descriptors magnitude is negligible. Quantifying the sensitivity of the descriptors to mixture quality, the sensitivity and intercept for linear least square curve fit along with the validity range for the 50 kWe load are consolidated in Table 13. It can be observed that PoPP and PRM10 indicate nearly the same sensitivity (they differ by an order of magnitude with factor 2) while the other two descriptors are nearly mixture quality independent, especially PoMHR. As for PoPP, while the sensitivity is not negligible, the fact that it is very much within the limit of cyclic dispersion permits treating PoPP to be mixture quality independent.

From the above analysis, it can be concluded that variations in mixture quality has limited/no impact on the combustion descriptors for producer gas fuelled operation.

Sensitivity of descriptors to end gas auto-ignition

Distortion of the pressure profile due to end gas auto-ignition (refer Fig. 3) manifests as deviations in the descriptor magnitude(s) which can be used as knock indicator(s). Sensitivity of various descriptors to pressure profile distortion and their ability to detect knock is examined in this section. Three end gas auto-ignition conditions representing incipient, established and heavy knock are considered for deriving the descriptors. The descriptors derived from four random knocking cycles are compared with normal operation descriptors as in Table 14.

Analysing the data in Table 14, no conclusive inference on knocking tendency can be drawn from PoPP. On the other hand, considerable differences in PoPPR and PoMHR can be observed for different knocking regimes. On the PoMBF50, when the end gas auto-ignites, heat release is near instantaneous and leads to a reduction in the overall burn duration. Accordingly, there is an overall shift in the mass burn fraction position(s) as evident from the listed values. Re-visiting PoPPR, PoMHR and PoMB-50, it can be observed that, with end gas auto-ignition, the descriptors experience a general deviation from normal combustion values, but do not indicate any particular sensitivity to the intensity of knock. On the other hand, PRM-10 indicates an increasing trend with knock intensity allowing to approximately identify the knock regime. Increase in PRM-10 with knock intensity is attributed to an increase in intensity of the pressure spikes at 10° aTDC (refer Fig. 3) leading to larger values of PRM-10.

Thus, PoMHR and PoMBF-50 along with PoPPR can be used for knock detection. PRM10 can be used to detect knock, as well as the knock regime.

Sensitivity of descriptors to gas composition

Having addressed in detail the combustion phasing for syngas composition typical of producer gas, the analysis is extended to four different syngas compositions with varying H_2 fraction. The two cylinder Cummins engine is operated with the

Table 12 – Sensitivity of descriptors for producer gas and gasoline operation.

Descriptor	NA	TA	Gas	NA ~ TA (%)	NA ~ gas (%)	TA ~ gas (%)
PoPP	−1.250	−0.764	−0.738	38.9	41.0	03.5
PoMBF50	−1.505	−1.359	−0.859	09.7	42.9	36.8
PoMHR	−2.000	−1.429	−0.887	28.6	55.7	37.9
PRM10	+0.050	+0.044	+0.037	10.8	26.7	17.8

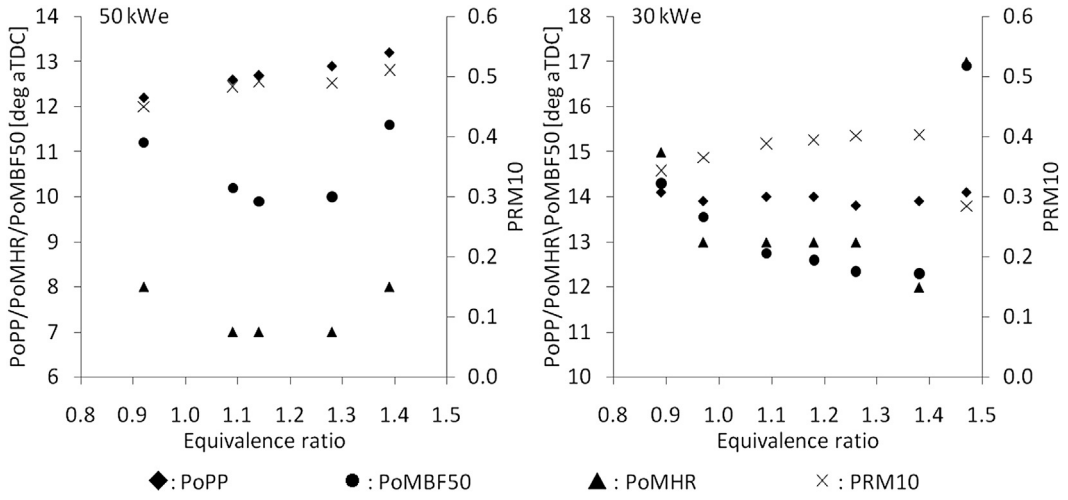

Fig. 11 – Sensitivity of descriptors to mixture quality.

four different compositions at a fixed load of 5.5 kWe, which corresponds to the peak load delivered by the engine with composition C1, the least energetic of the four compositions.

The preliminary feature that suggests potential influence on the combustion phasing is the heat release pattern. Fig. 12 compares the cumulative heat release pattern for the four different syngas compositions at the fixed load of 5.5 kWe and respective MBT ignition settings. Towards quantifying the differences, the various duration of heat release covering the initial and terminal burn phase are consolidated and presented as inset data.

It is evident from Fig. 12 that with increasing H_2 fraction, while the combustion duration for the 2–10% heat release regime decreases, duration for the 90–98% heat release regime increases. The reduction in the duration of initial phase of combustion is attributed to the higher laminar flame speed while the increase in duration of the terminal phase is attributed to the enhanced heat losses from the near wall mixtures due to higher thermal diffusivity and smaller flame quenching distance of mixtures containing H_2 [26]. This unequivocally establishes the influence of composition, especially H_2 on the combustion phasing.

Having identified and quantified the influence of composition on heat release pattern and because the foregone discussion relating to producer gas fuelled operation indicated the variation in sensitivity to ignition angle as one of the key features, the sensitivity of different combustion descriptors to ignition angle is identified by means of a spark sweep test with the four gas compositions.

The sensitivity of combustion descriptors to ignition angle for the four different gas compositions is consolidated in Table 15. It can be observed that with increasing hydrogen fraction in the mixture, the sensitivity to ignition angle increases. It must be noted that with an increase in the H_2 fraction in the mixture, while the sensitivity to heat loss increases, the fact that at 5.5 kWe, except for composition C1, operation with all other compositions pertains to part load operation. This effectively means a lower conversion efficiency. While these two factors could potentially represent the cause for the above behaviour, further analysis is required which is not in the scope of the current work.

Qualitative consolidation

Having established the combustion descriptors for producer gas in line with conventional fuels, a qualitative examination of the results is presented in Table 16.

The combustion descriptors are evaluated for independence to perturbations in mixture quality and load and the linearity of their response to change in ignition angle. The quality of the descriptor's response to parametric independence and linearity is presented using a combination of '+' and −. Symbolically, '+++' indicates the best case scenario (very high load/mixture quality independence and very high linearity) while '−−−' signifies the worst case. The experimental results indicate the response quality for producer gas (PG)

Table 13 – Quantification of descriptor sensitivity to mixture quality (at 50 kWe).

Descriptor = [Sensitivity]*phi + intercept

Descriptor	Sensitivity	Intercept	Range		Range magnitude	
			Low	High	Low	High
PoPP	+2.041	10.34	0.9	1.4	12.17	13.20
PoMHR	+0.000	07.00	1.1	1.3	07.00	07.00
PoMBF50	−0.859	11.12	1.1	1.3	10.18	10.00
PRM10	+0.114	00.35	0.9	1.4	00.45	00.51

Table 14 – Descriptors for knocking cycles.

	PoPP	PoPPR	PoMHR	PoMBF-50	PRM-10
Normal	**12.6**	**1.5**	**06.4**	**10.0**	**0.49**
Incipient knock	15.3	−1.5	14.0	5.0	0.65
	15.8	0.5	14.0	5.3	0.64
	15.4	1.5	05.0	7.0	0.61
	15.8	2.5	14.0	6.1	0.64
Established knock	12.5	8.5	10.0	5.1	0.74
	12.1	9.5	10.0	6.0	0.75
	12.7	8.5	10.0	6.0	0.72
	12.3	10.5	10.0	6.2	0.71
Heavy knock	10.2	8.5	08.0	4.0	0.95
	10.8	7.5	08.0	4.0	0.91
	10.4	8.5	08.0	4.6	0.89
	09.4	7.5	07.0	3.9	0.88

Bold values signify the magnitude of the descriptors for normal engine operation. The subsequent values are for abnormal combustion.

from the present work while the quality indicators for gasoline (G) are from the work of Pipitone [7].

It can be observed from Table 16 that;

1. The simulation trends, describing the parametric independence and linearity broadly match the experimental trends for both producer gas and gasoline. This justifies the utility of the Wiebe function based zero-dimensional model for the assessment of the combustion descriptors.
2. Over the broad agreement, differences are observed in load and ignition angle response for the position of peak pressure rise. Simulation results suggest a positive response, but experimental results indicate a negative response. This is argued to be due to the extreme sensitivity of the position of peak pressure rise, especially to the cycle to cycle variations. The number of cycles considered for ensemble averaging based on other descriptors is insufficient to average out the fluctuations of the position of peak pressure rise resulting in the difference between the experimental and simulation trends.
3. Experimental trends for both producer gas and gasoline indicate strong agreement with the identified requirement (parameter independence and linearity) as compared to simulation results. This response is attributed to the fact that the parametric range for experimental investigations is rather narrow as compared to the range considered for simulations. Actual engine operation parameter range is constrained by issues like end gas auto-ignition, cycle to cycle variations, etc.; while no such limitations exist for engine simulation, especially for zero-dimensional models. This permits adoption of a rather broad range of parameters for simulation studies.
4. Gasoline operation agrees strongly with the indicated conditions as compared to producer gas. This suggests higher sensitivity of producer gas to the parameters as compared to gasoline. This observation is consistent with the indications in Fig. 10 and Table 12.

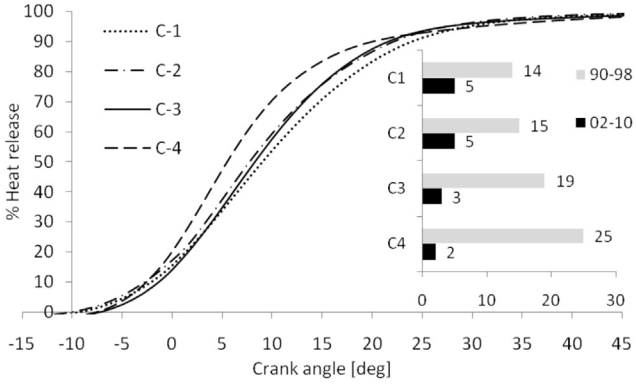

Fig. 12 – MBT heat release pattern for the four syngas compositions.

Table 15 – Combustion descriptors sensitivity to ignition timing for different syngas compositions.

	PoPP	PoMBF50	PoMHR	PRM10
C1	−1.01	−1.31	−1.52	0.030
C2	−1.13	−1.51	−1.74	0.041
C3	−1.28	−1.60	−1.93	0.054
C4	−1.36	−1.72	−2.21	0.061

Conclusions

Sensitivity of combustion phasing and descriptors to load, mixture quality and ignition timing for producer gas fuelled operation of a stationary multi-cylinder spark ignited engine is addressed. The thermo-kinematic response of the engine fuelled using gasoline and producer gas under NA and TA mode of operation have been quantified. The work represents a generic approach for arriving at combustion descriptors for engine operation with alternative fuels. Some of the key outcomes of the work are identified as below;

1. The validity of combustion descriptors as control parameters for engine control has been established based on numerical simulations and verified experimentally.
2. Spark sweep tests indicate retarded MBT ignition setting for producer gas operation, attributed mainly to the presence of H_2. The MBT peak load under NA mode is 27.3 kWe while it 72.8 kWe at a compressor pressure ratio of 2.2 for the TA mode of operation. The TA mode peak load represents a de-rating of about 19% from baseline diesel operation and is knock limited (due to CR reduction).
3. The mixture quality operating regime is positioned rich of stoichiometry especially at loads greater than 70%. The optimal operation mixture quality is at phi of 1.12 and is nearly load independent. The overall rich positioning is attributed to the influence of CO and H_2 as established by laminar flame speed calculations.
4. Sensitivity analysis based on simulation studies reveals that except for PoPPR the other pressure trace based descriptors remain broadly independent of mixture quality and load. All the descriptors indicate near linear response to change in the ignition angle.
5. It is observed that combustion for producer gas fuelled MBT operating conditions is advanced by a couple of degrees and is consistent with numerical simulation results.

Table 16 – Qualitative consolidation of descriptors response to load, mixture quality and ignition angle.

Descriptor	Simulation					Experiments		
	Mixture quality		Load	Ignition angle		Mixture quality	Load	Ignition angle
	m	DoC						
	Independence			Linearity		Independence		Linearity
PoPP	++	+++	++	++	PG	+++	+++	+++
					G	++	+++	+++
PoPPR	– – –	– – –	++	+	PG	– – –	––	––
					G	++	––	––
PoMHR	+	++	+++	+++	PG	++	++	+++
					G	++	+++	+++
PoMBF50	+	++	+++	+++	PG	–	++	++
					G	++	+++	+++
PRM10	+++	+	+++	++	PG	+++	++	++
					G	++	+++	+++

Further, it is observed that as the energy consumption per cycle approaches that of conventional fuels, the descriptors approach literature reported values.

6. While the combustion descriptors remain independent of mixture quality and load above 25% of the rated load, they respond linearly to change in ignition angle for producer gas fuelled operation consistent with simulation results.
7. It has been established that the descriptors remain independent of the cylinder from which the data has been acquired. This is concluded based on the absence of descriptor skewness in all the cylinders.
8. It has been established that knock detection, hitherto possible only by spectral analysis of pressure trace or dedicated sensors, is also possible using combustion descriptors (PoMHR, PoMBF-50 for knock detection and PRM10 for knock and regime detection).
9. Influence of H_2 fraction on the initial and terminal combustion phase and hence on the descriptor sensitivity to ignition has been quantified.

While the generic nature of the combustion phasing and combustion descriptors is similar to gasoline/natural gas fuelled engines, differences in factors like the absolute value of descriptors at MBT, sensitivity to ignition angle and shape factor, etc., demand a re-calibration of the control system for use in open loop control system on changing over from conventional fuelled operation to producer gas fuelled operation.

Acknowledgement

The work was supported by the Ministry of New and Renewable Energy, Government of India, New Delhi (3/3/2008 – R & D).

Nomenclature

η_{otto}	Otto cycle efficiency
Q_{cum}	cumulative heat supplied to the engine
$V(\theta)$	instantaneous volume
V_c	clearance volume
V_s	swept volume
0D	zero Dimensional
CoV	coefficient of Variation
DoCVC	degreesree of constant volume
LCV	lower calorific value
MBT	maximum brake torque
NA	naturally aspirated
NG	natural gas
PG	producer gas
PoMBF50	position of 50% mass burn fraction
PoMHR	position of maximum heat release
PoPP	position of peak pressure
PoPPR	position of peak pressure rise
SEC	specific energy consumption
SI	spark ignited
TA	turbocharged after-cooled
TDC	top dead center

REFERENCES

[1] Heywood John B. Internal combustion engine fundamentals, 930. New York: Mcgraw-hill; 1988.
[2] Hubbard M, Dobson PD, Powell JD. Closed loop control of spark advance using a cylinder pressure sensor. J Dyn Syst Meas Control 1976;98(4):414–20.
[3] Zhu Guoming G, Daniels Chao F, Winkelman James. MBT timing detection and its closed-loop control using in-cylinder pressure signal. No. 2003-01-3266. SAE Technical Paper; 2003.
[4] Zhu Guoming, Ibrahim Haskara, Jim Winkelman. Stochastic limit control and its application to spark limit control using ionization feedback. American Control Conference, 2005. Proceedings of the 2005. IEEE, 2005.
[5] Kawamura Yoshihisa, Shinshi M, Sato H, Takahashi N, Iriyama M. MBT control through individual cylinder pressure detection. No. 881779. SAE Technical Paper; 1988.
[6] Müller Rainer, Hart M, Truscott A, Noble A, Kroetz G, Eickhoff M, et al. Combustion pressure based engine management system. No. 2000-01-0928. SAE Technical Paper; 2000.
[7] Pipitone Emiliano. A comparison between combustion phase indicators for optimal spark timing. J Eng Gas Turbines Power 2008;130(5):052808.
[8] Cook Harvey A, Heinicke Orville H, Haynie William H. Spark-timing control based on correlation of maximum-economy spark timing, flame-front travel and cylinder-pressure rise.

No. NACA-886. Washington DC: National Aeronautics and Space Administration; 1947.
[9] Bargende Michael. Most optimal location of 50% mass fraction burned and automatic knock detection. Components for automatic optimization of SI-engine calibrations. M T Z 1995;56(10):632–8.
[10] Leonhardt Steffen, Muller Norbert, Isermann Rolf. Methods for engine supervision and control based on cylinder pressure information. IEEE/ASME Transactions Mechatronics 1999;4(3):235–45.
[11] Beccari A, Beccari S, Pipitone E. An analytical approach for the evaluation of the optimal combustion phase in spark ignition engines. J Eng Gas turbines power 2010;132(3):032802.
[12] Beccari A, Pipitone E. Proportional integral spark timing control by means of in-cylinder pressure analysis. FISITA 2004 [World Automotive Congress].
[13] Rassweiler Gerald M, Withrow Lloyd. Motion pictures of engine flames correlated with pressure cards. No. 380139. SAE Technical Paper; 1938.
[14] Matekunas Frederic A. Engine combustion control with dilution flow by pressure ratio management. U.S. Patent No. 4,624,229. 25 Nov. 1986.
[15] Matekunas, Frederic A. Engine combustion control with fuel balancing by pressure ratio management. U.S. Patent No. 4,621,603. 11 Nov. 1986.
[16] Matekunas, Frederic A. Engine combustion control with ignition timing by pressure ratio management. U.S. Patent No. 4,622,939. 18 Nov. 1986.
[17] Sellnau Mark C, Matekunas FA, Battiston PA, Chang C-F, Lancaster DR. Cylinder-pressure-based engine control using pressure-ratio-management and low-cost non-intrusive cylinder pressure sensors. No. 2000-01-0932. SAE Technical paper; 2000.
[18] Mobley Chris. Non-intrusive in-cylinder pressure measurement of internal combustion engines. No. 1999-01-0544. SAE Technical Paper; 1999.
[19] Astbury GR. A review of the properties and hazards of some alternative fuels. Process Saf Environ Prot 2008;86(6):397–414.
[20] Karim Ghazi A. Hydrogen as a spark ignition engine fuel. Int J Hydrogen Energy 2003;28(5):569–77.
[21] Ma Fanhua, Wang Y, Wang J, Ding S, Wang Y, Zhao S. Effects of combustion phasing, combustion duration, and their cyclic variations on spark-ignition (SI) engine efficiency. Energy & Fuels 2008;22(.5):3022–8.
[22] Shudo Toshio. Improving thermal efficiency by reducing cooling losses in hydrogen combustion engines. Int J Hydrogen Energy 2007;32(17):4285–93.
[23] D'Andrea T, Henshaw PF, Ting DS-K. The addition of hydrogen to a gasoline-fuelled SI engine. Int J Hydrogen Energy 2004;29(14):1541–52.
[24] Verhelst Sebastian, Wallner Thomas. Hydrogen-fueled internal combustion engines. Prog Energy Combust Sci 2009;35(6):490–527.
[25] Bradley Derek. "Problems of predicting turbulent burning rates. Combust Theory Model 2002;6(2):361–82.
[26] Shivapuji Anand M, Dasappa S. Experiments and Zero D modeling studies using specific Wiebe coefficients for producer gas as fuel in spark ignited engines. Proc Institution Mech Eng Part C: J Mech Eng Sci 2012. 0954406212463846.
[27] Ghojel JI. Review of the development and applications of the Wiebe function: a tribute to the contribution of Ivan Wiebe to engine research. Int J Engine Res 2010;11(4):297–312.
[28] Karim GA, Wierzba I, Al-Alousi Y. Methane-hydrogen mixtures as fuels. Int J Hydrogen Energy 1996;21(7):625–31.
[29] Li H, Karim GA. Experimental investigation of the knock and combustion characteristics of CH_4, H_2, CO, and some of their mixtures. Proc Institution Mech Eng Part A J Power Energy 2006;220(5):459–71.
[30] Porpatham E, Ramesh A, Nagalingam B. Effect of hydrogen addition on the performance of a biogas fuelled spark ignition engine. Int J Hydrogen Energy 2007;32(12):2057–65.
[31] Reed Thomas B. Biomass gasification. Principles and technology. Noyes Data Corporation; 1981.
[32] Sandeep K, Dasappa S. Oxy–steam gasification of biomass for hydrogen rich syngas production using downdraft reactor configuration. Int J Energy Res 2014;38(2):174–88.
[33] Mukunda HS. Understanding combustion. Universities Press (India) Private Limited Publication; 1989. p. 7371. ISBN 978.81.
[34] Quaak Peter, Knoef Harrie, Stassen Hubert E. Energy from biomass: a review of combustion and gasification technologies23. World Bank Publications; 1999.
[35] Kline S Jv, McClintock FA. Describing uncertainties in single-sample experiments. Mech Eng 1953;75(1):3–8.
[36] Holman JP. Experimental methods for engineers. New York: McGraw and Hill Inc.; 1994.
[37] Orhan Akansu S, Kahraman Nafiz, Ceper Bilge. Experimental study on a spark ignition engine fuelled by methane–hydrogen mixtures. Int J Hydrogen Energy 2007;32(17):4279–84.
[38] Devan PK, Mahalakshmi NV. Performance, emission and combustion characteristics of poon oil and its diesel blends in a DI diesel engine. Fuel 2009;88(5):861–7.
[39] Saravanan N, Nagarajan G. An experimental investigation of hydrogen-enriched air induction in a diesel engine system. Int J Hydrogen Energy 2008;33(6):1769–75.
[40] Kitagawa Toshiaki, Nakahara T, Maruyama K, Kado K, Hayakawa A, Kobayashi S. Turbulent burning velocity of hydrogen–air premixed propagating flames at elevated pressures. Int J Hydrogen Energy 2008;33(20):5842–9.
[41] Tang Chenglong, Huang Z, Wang J, Zheng J. Effects of hydrogen addition on cellular instabilities of the spherically expanding propane flames. Int J Hydrog energy 2009;34(5):2483–7.
[42] Lancaster David R, Krieger RB. Effects of turbulence on spark-ignition engine combustion. No. 760160. SAE Technical Paper; 1976.
[43] Lee Kihyung, Bae Choongsik, Kang Kernyong. "The effects of tumble and swirl flows on flame propagation in a four-valve SI engine. Appl Therm Eng 2007;27(11):2122–30.
[44] Dasappa S. On the estimation of power from a diesel engine converted for gas operation–a simple analysis. Power 2005;1:2.
[45] Shivapuji Anand M, Dasappa S. Selection and thermodynamic analysis of a turbocharger for a producer gas-fuelled multi-cylinder engine. Proc Institution Mech Eng Part A J Power Energy 2014;228(3):340–56.
[46] Badr OA, Elsayed N, Karim GA. An investigation of the lean operational limits of gas-fueled spark ignition engines. J energy Resour Technol 1996;118(2):159–63.
[47] Wang Jinhua, Chen H, Liu B, Huang Z. Study of cycle-by-cycle variations of a spark ignition engine fueled with natural gas–hydrogen blends. Int J hydrogen energy 2008;33(18):4876–83.
[48] Tanuma Takeshi, Sasaki K, Kaneko T. Ignition, combustion, and exhaust emissions of lean mixtures in automotive spark ignition engines. No. 710159. SAE Technical Paper; 1971.
[49] Quader Ather A. What limits lean operation in spark ignition engines-flame initiation or propagation?. No. 760760. SAE Technical Paper; 1976.
[50] Winsor Richard E, Patterson Donald J. Mixture turbulence-a key to cyclic combustion variation. No. 730086. SAE Technical Paper; 1973.
[51] Central Electricity Regulatory Commission, Government of India. Indian Electricity Grid Code (IEGC)-2010; 2010.

[52] Nakajima Y, Onoda M, Nagai T, Yoneda K. Consideration for evaluating knock intensity. JSAE Rev 1982;9:27–35.
[53] Kawahara Nobuyuki, Tomita Eiji. Visualization of auto-ignition and pressure wave during knocking in a hydrogen spark-ignition engine. Int J hydrogen energy 2009;34(7):3156–63.
[54] Kamimoto Take. In: Arcoumanis Constantine, editor. Flow and combustion in reciprocating engines. Springer; 2009.
[55] He Pingan, S. Jagannathan. Lean combustion stability of spark ignition engines. Control Applications, 2003. CCA 2003. Proceedings of 2003 IEEE Conference on. vol. 1. IEEE, 2003.
[56] Shudo Toshio, Nabetani Shigeki. Analysis of degree of constant volume and cooling loss in a hydrogen fuelled SI engine. No. 2001-01-3561. SAE Technical Paper; 2001.
[57] Shrestha SO Bade, Karim GA. Hydrogen as an additive to methane for spark ignition engine applications. Int J Hydrogen Energy 1999;24(6):577–86.
[58] Kee RJ, Rupley F, Miller J, Coltrin M, Grcar J, Meeks E, et al. CHEMKIN Release 4.1. San Diego, CA: Reaction Design; 2006.
[59] Saxena Priyank, Williams Forman A. Testing a small detailed chemical-kinetic mechanism for the combustion of hydrogen and carbon monoxide. Combust Flame 2006;145(1):316–23.
[60] Sun Hongyan, Yang S, Jomaas G, Law C. High-pressure laminar flame speeds and kinetic modeling of carbon monoxide/hydrogen combustion. Proc Combust Inst 2007;31(1):439–46.
[61] Hu Erjiang, Huang Z, He J, Jin C, Zheng J. Experimental and numerical study on laminar burning characteristics of premixed methane–hydrogen–air flames. Int J hydrogen energy 2009;34(11):4876–88.
[62] Ilbas M, Crayford A, Yılmaz I, Bowen P, Syred N. Laminar-burning velocities of hydrogen–air and hydrogen–methane–air mixtures: an experimental study. Int J Hydrogen Energy 2006;31(12):1768–79.
[63] Barnard, Allan John. Flame Combust 1985.
[64] Hernandez Juan J, Lapuerta M, Serrano C, Melgar A. "Estimation of the laminar flame speed of producer gas from biomass gasification. Energy & fuels 2005;19.5:2172–8.
[65] Ball JK, Raine RR, Stone CR. Combustion analysis and cycle-by-cycle variations in spark ignition engine combustion Part 1: an evaluation of combustion analysis routines by reference to model data. Proc Institution Mech Eng Part D J Automob Eng 1998;212(5):381–99.
[66] Ball JK, Raine RR, Stone CR. Combustion analysis and cycle-by-cycle variations in spark ignition engine combustion Part 2: a new parameter for completeness of combustion and its use in modelling cycle-by-cycle variations in combustion. Proc Institution Mech Eng Part D J Automob Eng 1998;212(6):507–23.
[67] Zhen Xudong, Wang Y, Xu S, Zhu Y, Tao C, Xu T, et al. The engine knock analysis–an overview. Appl Energy 2012;92:628–36.
[68] Ross Sheldon M. Introduction to probability and statistics for engineers and scientists. Academic Press; 2009.